ELSEVIER

www.elsevier.nl/locate/jorganchem

Journal of Organometallic Chemistry 599 (2000) 170–177

Journal of Organometallic Chemistry

C–F bond activation in polyfluorobenzothiolate compounds of Os(III). X-ray structures of $[Os(SC_6F_4(F\text{-}2))(SC_6F_5)_2(PMe_2Ph)_2]$, $[Os(SC_6F_5)_2(o\text{-}S_2C_6F_4)(PMe_2Ph)]$ and $[Os(C_6F_5)_2(o\text{-}S_2C_6F_4)(PMe_2Ph)_2]$

Maribel Arroyo [a], Sylvain Bernès [b], Jose Luis Brianso [c], Estela Mayoral [b], Raymond L. Richards [d], Jordi Rius [e], Hugo Torrens [b,*]

[a] *Centro de Química, Instituto de Ciencias, BUAP, Boulevard 14 Sur 6303, Cd. Universitaria, 72570 Puebla, Puebla, Mexico*
[b] *DEPg., F. de Química, Cd. Universitaria, 04510 Mexico D.F., Mexico*
[c] *Unidad de Cristalografia, F. de Ciencias, UAB, E-08193 Bellaterra, Spain*
[d] *John Innes Centre, Norwich Research Park, Colney, Norwich NR4 7UH, UK*
[e] *Institut de Ciencia de Materials de Barcelona, Campus de la UAB, E-08193 Bellaterra, Spain*

Received 7 April 1999; received in revised form 9 December 1999

Abstract

Thermolysis of $[Os(SR)_3(PMe_2Ph)_2]$ ($R = C_6F_5$ (**1a**) or C_6HF_4-4 (**1b**)) in refluxing toluene affords $[Os(SC_6F_5)_2$-$(o\text{-}S_2C_6F_4)(PMe_2Ph)]$ (**2a**), $[Os(SC_6HF_4)_2(o\text{-}S_2C_6HF_3)(PMe_2Ph)]$ (**2b**), and $[Os(C_6F_5)_2(o\text{-}S_2C_6F_4)(PMe_2Ph)_2]$ (**3a**) through processes involving C–F and C–S bond cleavage as well as rearrangement of C–S bonds. The single-crystal diffraction structures of **1a**, **2a** and **3a** have been determined. In the solid state compound **1a** shows a C–F → Os interaction.

Keywords: C–F bond activation; Polyfluorobenzothiolate; Osmium; Thermolysis

1. Introduction

The activation of fluorinated hydrocarbons by metal centres has been an area of intense study during the last decade [1–9]. Structural reports of transition-metal complexes with carbon–fluorine–metal interactions [10,11] as well as research focused on carbon–fluorine bond activation [12–14] have been reviewed recently.

Previously, we have reported the synthesis of $[M(SC_6F_5)_3(PMe_2Ph)_2]$ (M = Ru, Os) and the X-ray structure of the ruthenium compound, showing that this complex bears a C–F–Ru interaction in the solid state [15,16]. The X-ray structure of the osmium compound has also been published as a preliminary report [17].

We have now found that thermolysis of $[Os(SR)_3(PMe_2Ph)_2]$ ($R = C_6F_5$ (**1a**) or C_6HF_4-4 (**1b**)) in refluxing toluene causes a substantial rearrangement–oxidative reaction giving rise to a complex mixture of products from which the Os(IV) complexes $[Os(SC_6F_5)_2(o\text{-}S_2C_6F_4)(PMe_2Ph)]$ (**2a**), $[Os(SC_6HF_4\text{-}4)_2(o\text{-}S_2C_6HF_3)(PMe_2Ph)]$ (**2b**) and $[Os(C_6F_5)_2(o\text{-}S_2C_6F_4)(PMe_2Ph)_2]$ (**3a**) have been isolated. Compounds **1a**, **2a** and **3a**, have been structurally characterised.

2. Results and discussion

The synthesis of the formally pentaco-ordinated, Os(III) d^5 complexes $[Os(SR)_3(PMe_2Ph)_2]$ ($R = C_6F_5$ (**1a**) or C_6HF_4-4 (**1b**)) has been previously reported [15,16]. Since $[Ru(SC_6F_5)_3(PMe_2Ph)_2]$ has been shown to have a Ru–F–C interaction, we carried out an X-ray diffraction molecular structure determination of

* Corresponding author. Fax: +52-5-6223724.
E-mail address: torrens@servidor.unam.mx (H. Torrens)

0022-328X/00/$ - see front matter
PII: S0022-328X(99)00760-3

$[Os(SC_6F_5)_3(PMe_2Ph)_2]$ (**1a**) in a search for a similar bond. The molecular structure of **1a** is shown in Fig. 1, and selected bond distances and angles are collected in Table 1.

The important feature of this structure is the interaction of an *ortho*-fluorine of one of the SC_6F_5 ligands with the metal to create an S–F chelate ligand, thus achieving six coordination in an approximately octahedral arrangement. The Os–F distance of 2.531(6) Å is shorter than the calculated van der Waals distance [18,19] (3.1 Å) and implies a moderate bond strength of this three-centre, four-electron C–F–Os bond.

Metal–fluorine distances in C–F–M bonds span from 2.15 to 3.30 Å, between 24 and 8% shorter than the sum of fluorine and metal van der Waals radii [10,11]. Therefore, the Os–F distance of 2.531(6) Å found in **1a** lies at the lower end of this scale and it is almost 19% shorter than the corresponding van der Waals distance.

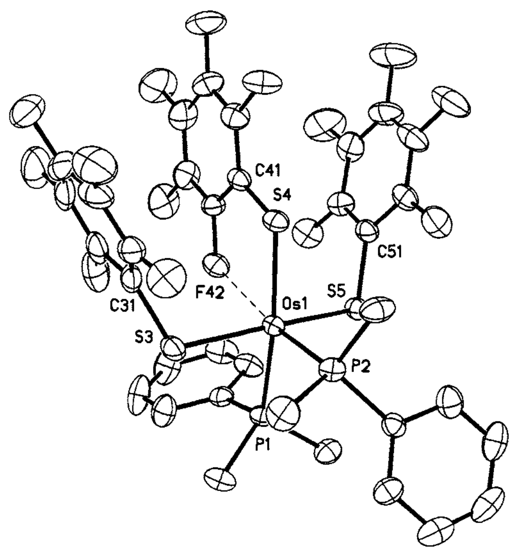

Fig. 1. Structure of $[Os(SC_6F_4(F\text{-}2))(SC_6F_5)_2(PMe_2Ph)_2]$ (**1a**). (Ellipsoids at 30% probability levels. Hydrogen atoms were omitted for clarity.)

Table 1
Bond lengths (Å) and angles (°) of $[Os(SC_6F_5)_3(PMe_2Ph)_2]$ (**1a**)

Distances		Angles	
Os-P1	2.352(2)	S4–Os–F42	76.36(11)
Os–P2	2.274(2)	S5–Os–F42	86.31(13)
Os–S3	2.327(2)	S3–Os–F42	83.53(13)
Os–S4	2.415(2)	P2–Os–F42	170.86(11)
Os–F42	2.531(5)	P1–Os–F42	94.45(11)
Os–S5	2.328(2)	P2–Os–S3	97.33(8)
S3–C31	1.769(9)	S3–Os–S5	165.55(8)
S4–C41	1.765(8)	P1–Os–S4	170.81(7)
S5–C51	1.795(8)	P1–Os–P2	94.69(8)

A further feature of this structure is that the C_6F_5 groups attached to S(3) and S(5) are eclipsed about the S···S vector; they are thus aligned with the central chelating ligand to form, as closely as possible, a stacked pattern.

In exploring the reactivity of compounds **1a**–**b** we have found that in refluxing dry toluene under nitrogen, $[Os(SR)_3(PMe_2Ph)_2]$ ($R = C_6F_5$ (**1a**) or C_6HF_4-4 (**1b**)) is involved in thermolysis reactions. The original dark purple solutions slowly turn green and the chromatographic resolution of the final mixtures gives rise to two, from **1a**, or one, from **1b**, distinct, highly coloured fractions.

Additionally, GLC–mass spectrometry analyses of the solvent indicate the presence of C_6HF_5 and $C_6H_2F_4$ from the reactions of **1a** and **1b**, respectively. As discussed below, three of the reaction products have been identified according to the following reactions:

$[Os(SC_6F_5)_3(PMe_2Ph)_2]$ **(1a)**

$\rightarrow [Os(SC_6F_5)_2(o\text{-}S_2C_6F_4)(PMe_2Ph)]$ (**2a**)

$+ [Os(C_6F_5)_2(o\text{-}S_2C_6F_4)(PMe_2Ph)_2]$ (**3a**)

$[Os(SC_6HF_4\text{-}4)_3(PMe_2Ph)_2]$ (**1b**)

$\rightarrow [Os(SC_6HF_4\text{-}4)_2(o\text{-}S_2C_6HF_3)(PMe_2Ph)]$ (**2b**)

Complexes $[Os(SC_6F_5)_2(o\text{-}S_2C_6F_4)(PMe_2Ph)]$ (**2a**) and $[Os(SC_6HF_4)_2(o\text{-}S_2C_6HF_3)(PMe_2Ph)]$ (**2b**) are dark green, crystalline solids. The FAB mass spectra of both compounds show the corresponding parent ions (**2a** $m/z = 940$, 68%; **2b** $m/z = 886$, 92%) from which successive losses of SC_6F_5 and C_6HF_5 or SC_6HF_4-4 and $C_6H_2F_4$ (**2a** $m/z = 741$, 22% and 573, 12%; **2b** $m/z = 705$, 44% and 555, 16%) are observed. The loss of C_6F_5 or C_6HF_4-4 from the parent ions is also observed. A common signal in both spectra is that corresponding to PMe_2Ph^+.

2.1. Crystal structure of $[Os(SC_6F_5)_2(o\text{-}S_2C_6F_4)(PMe_2Ph)]$ (2a)

The molecular structure of $[Os(SC_6F_5)_2(o\text{-}S_2C_6F_4)(PMe_2Ph)]$ (**2a**) is shown in Fig. 2 and selected bond distances and angles are collected in Table 2.

The structure of **2a** shows an essentially trigonal-bipyramidal coordination geometry with an axial PMe_2Ph group. The quelating dithiolate ligand occupies both axial and equatorial positions with two equatorial $(SC_6F_5)^-$ moieties. The structure of **2a** resembles those of $[OsCl(SC_6F_5)_3(PMe_2Ph)]$ [20], $[Os(SC_6HF_4\text{-}4)_4(PPh_3)]$ [21] and $[OsCl(SC_6F_5)_2(SC_6H_4(CF_3)\text{-}3)(PMe_2Ph)]$ [21]. As might be expected [22], the axial Os–S distance (2.381(3) Å) is longer than the mean equatorial Os–S distance (2.207(3) Å). The angles around the sulphur atoms show considerable variations, thus one thiolate shows a substantial distortion

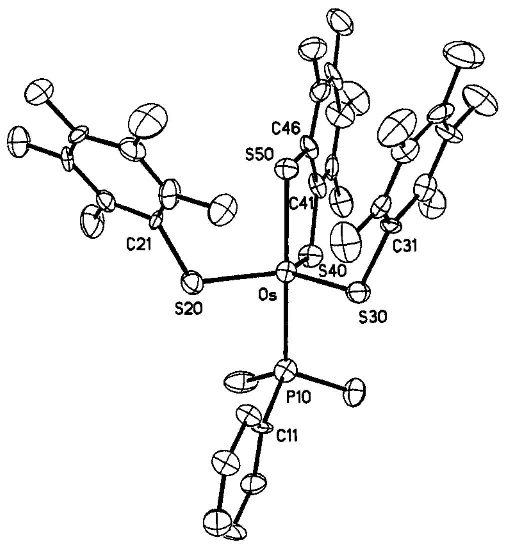

Fig. 2. Structure of $[Os(SC_6F_5)_2(o\text{-}S_2C_6F_4)(PMe_2Ph)]$ (**2a**). (Ellipsoids at 30% probability levels. Hydrogen atoms were omitted for clarity.)

Table 2
Bond lengths (Å) and angles (°) of $[Os(SC_6F_5)_2(o\text{-}S_2C_6F_4)(PMe_2Ph)]$ (**2a**)

Distances		Angle	
Os–S20	2.207(3)	S40–Os–S20	121.10(13)
Os–S30	2.213(3)	S40–Os–S30	118.84(13)
Os–S40	2.200(3)	S30–Os–S20	119.40(13)
Os–S50	2.381(3)	S40–Os–S50	87.76(12)
Os–P10	2.374(4)	S20–Os–S50	94.11(12)
P10–C11	1.823(7)	S30–Os–S50	96.27(13)
S20–C21	1.765(11)	S20–Os–P10	87.27(12)
S30–C31	1.761(11)	S30–Os–P10	87.75(13)
S40–C41	1.740(12)	S40–Os–P10	86.88(13)
S50–C46	1.749(11)	S50–Os–P10	174.40(13)

towards planarity, –C(21)–S(20)–Os 116.2(4)°, when compared to the second thiolate, –C(31)–S(30)–Os 111.7(4)°. At the dithiolate ligand, both these angles are closer to tetrahedral rather than to planar, –C(41)–S(40)–Os 107.8(5)° and C(46)–S(50)–Os 102.5(5)°. The tendency towards planarity around sulfur atoms has been previously associated with a substantial contribution to metal-sulfur π-bonding discouraging inversion of configuration and free metal-sulfur bond rotation [23].

On the other hand, there is no significant difference in equatorial Os–S distances from S-thiolate and S-dithiolate ligands.

The dithiolate ligand $(S_2C_6F_4)^{2-}$ forms a five-membered quelated ring with the osmium atom and the plane defined by the $OsS(40)S(50)C_6F_4$ moiety is the plane bisecting the S20–Os–S30 angle.

Variable-temperature ^{19}F-NMR of compounds **2a** and **2b** shows these molecules to be fluxional. At high temperature (ca. 80°C) the ^{19}F-NMR spectra of compound **2a**, Fig. 3, showed three signals (A_2BC_2 magnetic system, intensities 4:2:4) corresponding to the *ortho*-, *para*-and *meta*-fluorine nuclei of two magnetically equivalent $(SC_6F_5)^-$ substituents and four additional absorptions (Intensities 1:1:1:1) arising from each of the four distinct fluorine nuclei at the $(S_2C_6F_4)^{2-}$ moiety (ABCD magnetic system). As the temperature is decreased, the *ortho* and *meta* signals from the thiolate groups broaden (ca. 40°C) and eventually collapse (ca 20°C) giving rise, each one, to a pair of signals with the same intensity which at lower temperatures (ca. −40°C) reach their maximum definition without further changes. It is important to notice that the *para* signal remains unaffected during the process.

Except for small variations due to subtle changes in magnetic couplings, the sub-spectra arising from the dithiolate fragment remains essentially unchanged through the full range of temperatures.

As suggested by the results from NMR experiments, the fluxional behaviour of these complexes can be attributed to a restricted C–S(thiolate) bond rotation on this geometry.

Although a completely equivalent set of ^{19}F-NMR results is obtained when $[Os(SC_6HF_4\text{-}4)_2(o\text{-}S_2C_6HF_3)(PMe_2Ph)]$ (**2b**) is examined for fluxionality, indicating also that the $S–C_6HF_4$-4 bonds are not free to rotate, the ^{19}F-NMR data show that $[Os(SC_6HF_4\text{-}4)_2(o\text{-}S_2C_6HF_3)(PMe_2Ph)]$ exists as the pair of structural isomers shown below:

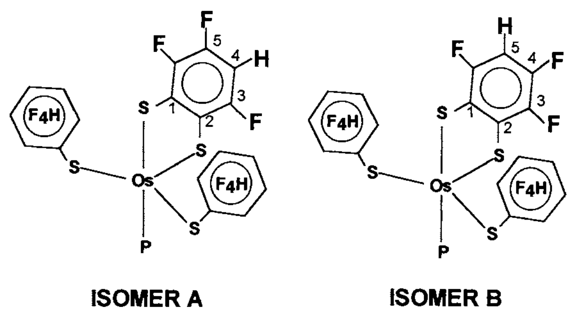

Both isomers differ in the relative position of the hydrogen atom at the dithiolate ring either attached to carbon 4 or carbon 5 relative to the axial sulfur atoms. At room temperature both isomers are present with a proportion of 4 to 1 (H-C4 to H-C5, respectively).

As expected, ^{31}P-NMR spectra of compounds **2a** and **2b** exhibit multiplets due to $P(CH_3)_2$ coupling (see Fig. 4). However, $^{31}P\text{-}\{^1H\}$-NMR spectra show one doublet for compound **2a** and one doublet for each of the two isomers of compound **2b**. Two-dimensional HETCOR $^{31}P\text{-}^{19}F$-NMR experiments indicate a relatively long-range '*trans*' phosphorus–fluorine magnetic coupling with $^5J_{P-F} = 8$Hz, $S_2C_6F_4$ (**2a**), $^5J_{P-F} = 7.8$Hz, $S_2C_6F_3H$-4 (**2b**, isomer A) and $^5J_{P-F} = 7.8$Hz, $S_2C_6F_3H$-5 (**2b**, isomer B). See Fig. 4.

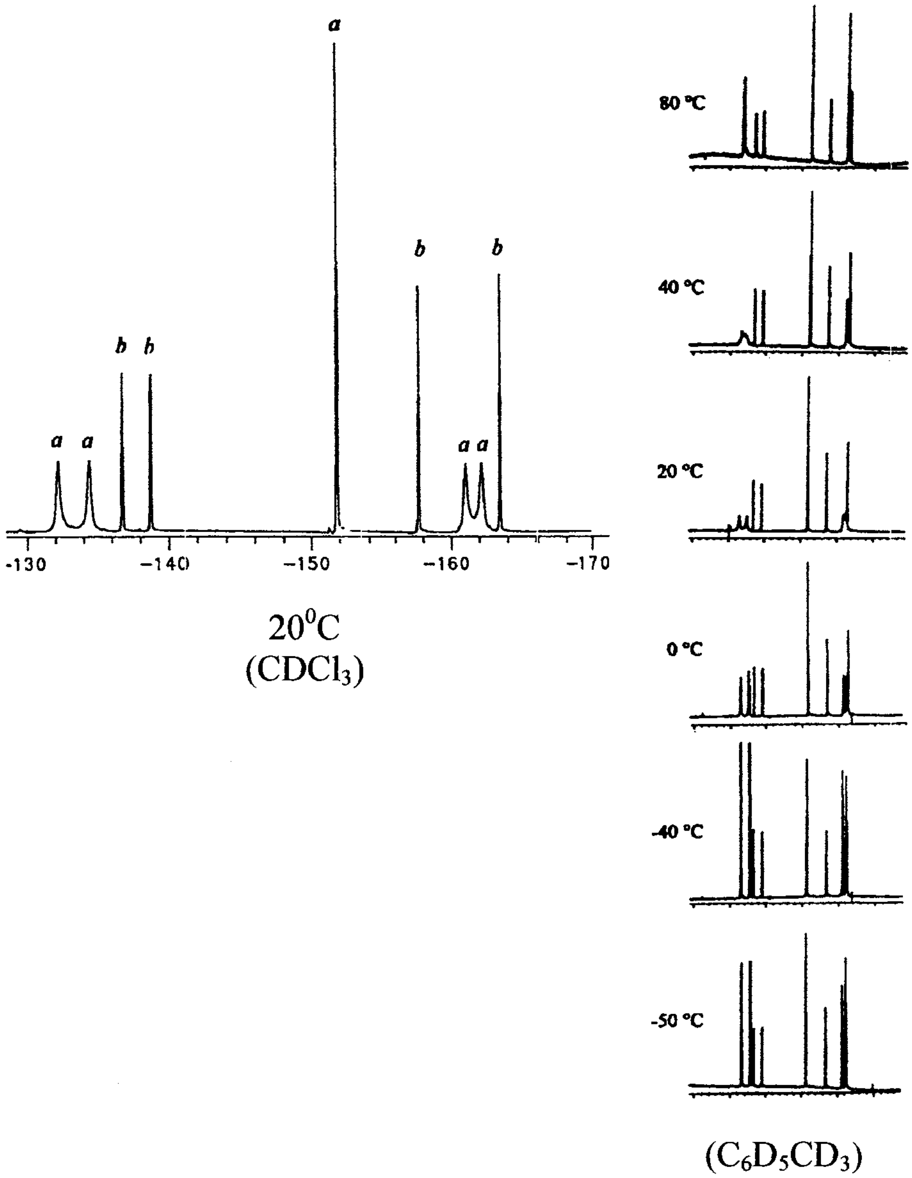

Fig. 3. Variable-temperature [19]F-NMR of $[Os(SC_6F_5)_2(o\text{-}S_2C_6F_4)(PMe_2Ph)]$ (**2a**). Signals a from $SC_6F_5^-$, signals b from $S_2C_6F_4^{2-}$.

Apparently, as a result of mesomeric effects, the exchange of positions between H–C4 and H–C5 in isomers A and B inverts the relative chemical-shift order of the fluorine nuclei. Thus, for isomer A, δF3 and δF5 are larger than δF6, whereas for isomer B, δF6 is larger than δF4 and δF3.

The activation energies for rotation about the S–C_6F_5 in **2a** and S–C_6HF_4-4 in **2b** are the same within experimental error. These ΔG^A are calculated to be 58.85 ± 4 kJ mol^{-1}, slightly higher than those found for P–C_6F_5 [24].

The complex $[Os(C_6F_5)_2(o\text{-}S_2C_6F_4)(PMe_2Ph)_2]$ (**3a**) is a red crystalline solid. The FAB mass spectrum of this compound shows the corresponding parent ion from which successive losses of C_6F_5 and PMe_2Ph follow.

2.2. Crystal structure of $[Os(C_6F_5)_2(o\text{-}S_2C_6F_4)(PMe_2Ph)_2]$ (3a)

The molecular structure of $[Os(SC_6F_5)_2(o\text{-}S_2C_6F_4)(PMe_2Ph)_2]$ is shown in Fig. 5 and selected bond distances and angles are collected in Table 3.

The structure of **3a** shows an essentially octahedral coordination geometry with *trans* phosphine ligands (P(20)–Os–P(30) 176.74(8)°). The quelating dithiolate ligand displays an angle of S(17)–Os–S(10) 86.63(8)°. The angles around the sulfur atoms Os–S(10)–C(11) 105.52(25), Os–S(17)–C(16), 106.93(25) suggest that the dithiolate sulfur atoms are nearly tetrahedral (109°).

Room-temperature [19]F-NMR spectra of compound $[Os(C_6F_5)_2(o\text{-}S_2C_6F_4)(PMe_2Ph)_2]$ (**3a**) show seven

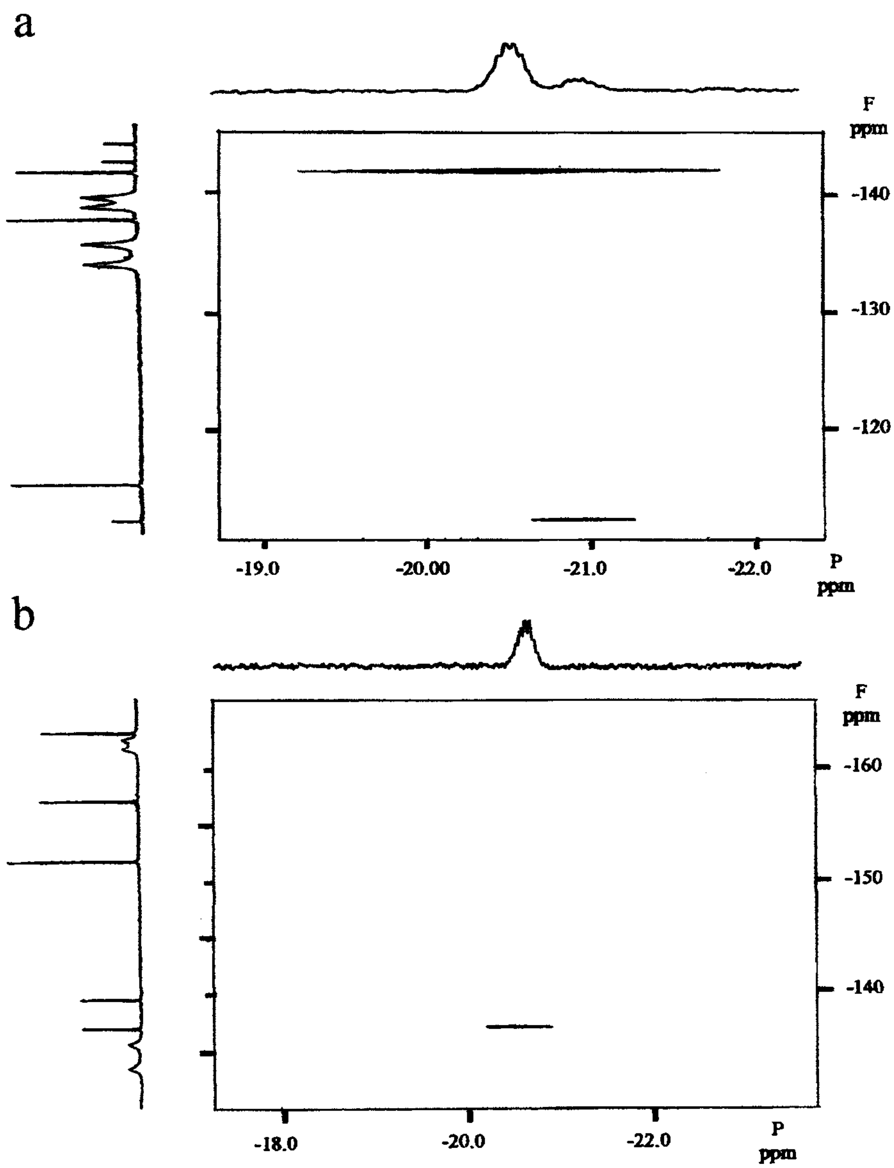

Fig. 4. HETCOR ^{31}P-^{19}F-NMR experiments of (a) $[Os(SC_6F_4H\text{-}4)_2(o\text{-}S_2C_6HF_3)(PMe_2Ph)_2]$ (**2b**) and (b) $[Os(SC_6F_5)_2(o\text{-}S_2C_6F_4)(PMe_2Ph)_2]$ (**2a**) (in C_6D_6).

equally intense resonances corresponding to the seven distinct fluorine atoms as found on the solid-state structure. Two of these signals arise from fluorine atoms at the dithiolate ligand and five additional signals arise from two C_6F_5 rings, each ring bearing distinct *ortho*- and *meta*-fluorine substituents.

Variable-temperature ^{19}F-NMR spectra of **3a** show no signs of fluxionality for this molecule from − 30 to 50°C. These results suggest that the C_6F_5 rings remain rigid, as found in the solid-state structure, probably because the relatively large PMe_2Ph ligands hinder the Os–C free rotation. As expected, the ^{31}P-{^1H}-NMR spectra of **3a** at room temperature show a single resonance.

The formation of the Os(IV) complexes $[Os(SC_6F_5)_2(o\text{-}S_2C_6F_4)(PMe_2Ph)]$ (**2a**) or $[Os(SC_6HF_4\text{-}4)_2(o\text{-}S_2C_6HF_3)(PMe_2Ph)]$ (**2b**) from the thermolysis of $[Os(SC_6F_5)_3(PMe_2Ph)_2]$ or $[Os(SC_6HF_4\text{-}4)_3(PMe_2Ph)_2]$, involves phosphine dissociation, cleavage of an *ortho*-carbon–fluorine bond at a thiolate ligand, transfer of a sulfur atom (and therefore carbon–sulfur bond splitting) and oxidation of the metal centre.

A C–F–Os interaction is expected to induce an activated *ortho*-C–F bond, bearing an electrophilic carbon atom. Such interactions are known to render C–F bonds highly susceptible to nucleophilic attack. Therefore the *ortho*-carbon atom can be envisaged as the centre of such a nucleophilic reaction with a thiolate–sulfur atom.

Nucleophilic displacement of *ortho*-fluorine from perfluorinated aromatic ligands attached to transition metals has been observed in a few examples where the C_6F_5 ring is bound to carbon or phosphorus atoms

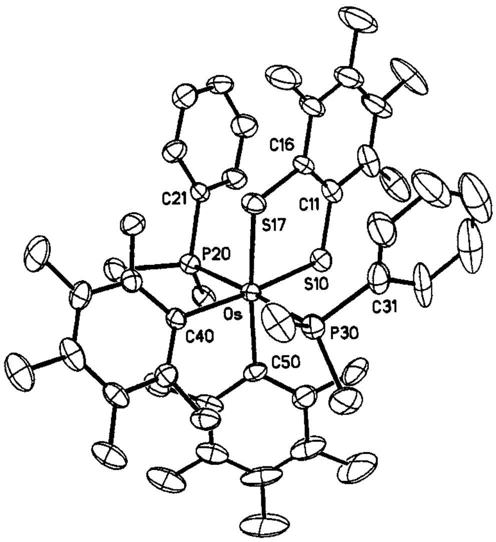

Fig. 5. Structure of $[Os(C_6F_5)_2(o\text{-}S_2C_6F_4)(PMe_2Ph)_2]$ (**3a**), (Ellipsoids at 30% probability levels. Hydrogen atoms were omitted for clarity.)

Table 3
Bond lengths (Å) and angles (°) of $[Os(C_6F_5)_2(o\text{-}S_2C_6F_4)(PMe_2Ph)_2]$ (**3a**)

Distances		Angles	
C40–Os	2.170(7)	P30–Os–C40	86.15(21)
C50–Os	2.182(8)	P30–Os–C50	92.07(22)
S17–Os	2.281(2)	P30–Os–S17	86.11(9)
S10–Os	2.286(2)	P30–Os–S10	97.51(9)
P20–Os	2.428(2)	P30–Os–P20	176.74(8)
P30–Os	2.429(3)	Os–S10–C11	105.52(25)
S10–C11	1.734(9)	Os–S17–C16	106.93(25)
S17–C16	1.707(8)	S10–Os–C40	175.53(21)
C16–C11	1.394(7)	S17–Os–C50	175.59(22)
P30–C31	1.814(7)	S17–Os–S10	86.63(8)
P20–C21	1.829(5)	C40–Os–C50	92.81(28)
C42–F42	1.341(7)	S17–Os–C40	91.07(20)
		S17–Os–C50	175.59(22)
		S10–Os–C50	89.63(21)

[25–27]. On the other hand, migration of a C_6F_5 group from a phosphine to Ir [28] and from a thiolate to Rh [29] has been reported.

The mechanism of these reactions has not been established but, since the products bear *ortho*-tetrafluorobenzene-dithiolate or *ortho*-trifluorobenzene-dithiolate ligands, one of the original thiolate moieties had to be involved in a reaction such that an *ortho*-fluorine atom is replaced by sulfur.

3. Experimental

All manipulations were carried out under dry oxygen-free dinitrogen atmospheres using Schlenk-tube techniques. Toluene was dried and degassed using standard techniques; thin-layer chromatography (TLC) (Merck, 5 × 7.5 cm^2 Kiesegel 60 F_{254}) was used when possible to monitor the progress of the reaction under study.

Complexes were characterised by IR spectra recorded over the 4000–200 cm^{-1} range on a Perkin–Elmer FTIR-1600, as CsI pellets.

^1H-, ^{19}F-, ^{31}P-{^1H} and HETCOR ^{19}F-^{31}P-NMR spectra were measured with a SDS-360 MHz and a modified NT-360 spectrometer operating at 360, 338 and 145 MHz, respectively by Spectral Data Services Inc. (IL, USA); chemical shifts are relative to TMS $\delta = 0$ (^1H), $CFCl_3$ $\delta = 0$ (^{19}F) and H_3PO_4 $\delta = 0$ (^{31}P). A standard variable-temperature unit was used to control the probe and it was checked periodically by a thermocouple to ensure that the temperature readings were within ±1°C. Complexes were studied in $C_6D_5CD_3$, C_6D_6 and $CDCl_3$.

Elemental analyses were determined by Galbraith Labs., USA.

FAB spectra were obtained on a JEOL JMS SX102-A mass spectrometer operated at an accelerating voltage of 10 kV. Samples were desorbed from 3-nitrobenzyl alcohol matrix using 3keV xenon atoms. Mass measurements in FAB are performed at 3000 resolution using magnetic field scans and the matrix ions as the reference material, or electric field scans with the sample peak bracketed by two (polyethylene glycol or cesium iodide) reference ions. $[Os(SR)_3(PMe_2Ph)_2]$ ($R = C_6F_5$ (**1a**) or C_6HF_4 (**1b**)) were prepared according to the literature methods [18,19].

3.1. Reaction of $[Os(SC_6F_5)_3(PMe_2Ph)_2]$ (1a)

$[Os(SC_6F_5)_3(PMe_2Ph)_2]$ (**1a**), (0.2 mmol), was dissolved in toluene (25 cm^3). The deep purple solution was kept under reflux for 9 h. The colour of the solution slowly changed from purple to green. The solvent was distilled off under vacuum. The solid product was purified trough a chromatographic column eluted with 10:1 hexane–dichloromethane. Two fractions were separated and dried under vacuum at room temperature for 4 h. Analyses and yield are as follow: **2a**, yield 20%; green, m.p. 200–204°C, decomposes, Anal. Calc.(%): C, 33.3; H, 1.2; S, 13.7: Found: C, 33.2; H, 1.1; S, 13.8. ^1H-RT-NMR, $CDCl_3$, phosphine, $\delta = 7.96$, m, 2H, PPh; $\delta = 7.58$, m, 3H, PPh; $\delta = 2.62$, d, 6H, PCH_3; $^2J_{H-P} = 9.8$ Hz. ^{19}F-RT-NMR, $C_6D_5CD_3$, thiolate, $\delta = -133.00$, br m, $2F_o$; $\delta = -135.2$, br m, $2F_o$; $\delta = -152.12$, br t, $2F_p$; $\delta = -161.90$, br m, $2F_m$; $\delta = -162.7$, br m, $2F_m$; $^3J_{m-p} = 20.96$ Hz; dithiolate, $\delta = -136.91$, pq, $1F_o$; $\delta = -139.30$, dd, 1F; $\delta = -157.32$, t, 1F; $\delta = -163.02$, t, 1F; $^3J_{F3-F4} = 22.2$, $^4J_{F3-F5} = 12.1$, $^3J_{F4-F5} = 21.45$, $^4J_{F4-F6} = 10.64$, $^3J_{F5-F6} = 21.11$ Hz. ^{31}P-RT-NMR, $C_6D_5CD_3$, $\delta = -20.31$, d; $^5J_{P-F6} = 8.76$ Hz.

3.2. Compound **3a**

Yield 17%; red, m.p. 160–170°C, Anal. Calc.: C, 40.3; H, 2.2; S, 6.3; Found: C, 40.2; H, 2.1; S, 5.6%. ^{19}F-RT-NMR, CD_3COCD_3, $\delta = -143.7$, m, 2F; $\delta = -160.48$, t, 2F; $\delta = -161.13$, m, 2F; $\delta = -164.07$, t, 2F; $\delta = -164.83$, t, 2F; $\delta = -177.52$, d, 2F; $\delta = -190.0$, d, 2F. ^{31}P-RT-NMR, CD_3COCD_3, $\delta = 41.5$, s.

3.3. Reaction of $[Os(SC_6HF_4)_3(PMe_2Ph)_2]$ (**1b**)

As described above, yielding **2b** after refluxing for 48 h, yield 17%; green, m.p. 205–210°C, decompose. Anal. Calc.: C, 35.3; H, 1.6; S, 14.5; Found: C, 35.6; H, 1.6; S, 14.4%. ^{1}H-RT-NMR, $CDCl_3$, isomer A, phosphine, $\delta = 7.99$, m, 8H, PPh; $\delta = 7.58$, m, 12H, PPh; $\delta = 2.62$, d, 24H, PCH_3, $\delta = 6.81$, m, 4H, dithiolate; $\delta = 7.01$, m, 8H, thiolate; $^2J_{H-P} = 9.8$ Hz; isomer B, phosphine, $\delta = 7.99$, m, 2H, PPh; $\delta = 7.58$, m, 3H, PPh; $\delta = 2.64$, d, 6H, PCH_3; $\delta = 6.81$, m, 1H, dithiolate; $\delta = 7.01$, m, 4H, thiolate; $^2J_{H-P} = 9.6$ Hz, ^{19}F-RT-NMR, $C_6D_5CD_3$, numbering as in diagram 1, isomer A, dithiolate, $\delta = -114.94$, pt, 0.8F6; $\delta = -138.24$, dd, 0.8F3; $\delta = -142.08$, br m, 0.8F5; $^3J_{F5-F6} = 21.0$, $^4J_{F3-F5} = 9.54$ Hz; thiolate, $\delta = -133.84$, br m, $2F_o$; $\delta = -135.63$, br m, $2F_o$; $\delta = -139.15$, br m, $2F_m$; $\delta = -140.04$, br m, $2F_m$; isomer B, dithiolate, $\delta = -111.78$, m, 0.2F6; $\delta = -142.9$, m, 0.2 F3; $\delta = -144.5$, dd, 0.2F4; thiolate, $\delta = -133.84$, br m, $2F_o$; $\delta = -135.63$, br m, $2F_o$; $\delta = -139.15$, br m, $2F_m$; $\delta = -140.04$, br m, $2F_m$. ^{31}P-RT-NMR, $C_6D_5CD_3$, isomer A, $\delta = -20.14$, br m, 4P; $^5J_{P-F} = 7.8$ Hz; isomer B, $\delta = -20.58$, br m, 1P; $^5J_{P-F} = 7.8$ Hz.

3.4. Crystal data: $[\overline{Os(SC_6F_4(F}\text{-}2))(SC_6F_5)_2(PMe_2Ph)_2]$ (**1a**)

$C_{34}H_{22}F_{15}OsP_2S_3$, M = 1063.8, orthorhombic, space group *Pbca*, $a = 18.142(3)$, $b = 18.064(2)$, $c = 22.954(3)$ Å, $U = 7522.5(19)$ Å^3, $Z = 8$, $T = 293(2)$ K, $D_c = 1.879$ g cm^{-3}, $F(000) = 4120$, μ(Mo–K$_\alpha$) = 3.74 mm^{-1}, λ(Mo–K$_\alpha$) = 0.71073 Å. The crystals are deep blue regular prisms. Intensity data were collected for a crystal of dimensions 0.40 × 0.35 × 0.15 mm mounted on a Siemens P4 diffractometer using Mo–K$_\alpha$ radiation. One octant including redundant data was collected to $\theta_{max} = 23°$ in a $\theta/2\theta$ scan mode at variable speed, between 3 and 60° min^{-1} ($-1 \leq h \leq 19$, $-1 \leq k \leq 19$, $-25 \leq l \leq 1$, 6327 reflections). Lorentz polarisation and absorption corrections were applied (42 ψ-scans, transmission factors in the range 0.188–0.350), yielding 5200 unique reflections ($R_{int} = 4.24\%$). The structure was solved from a Patterson map interpretation and refined by full-matrix least-squares on F^2 using the SHELXTL-93 program [30]. Hydrogen atoms were included on idealised positions and refined using a riding model. No significant features were observed on the last difference map (largest peak: 0.81 e Å^{-3}).

The anisotropic refinement was performed without constraints or restraints for 497 parameters and converged at $R_1 = 0.0402\%$ for 3496 data having $F > 4\sigma(F)$ and $wR_2 = 0.103\%$ for all data with $w = [\sigma^2(F_o^2) + (0.0511P)^2 + 0.00P]^{-1}$, $P = (\max\ [F_o^2, 0] + 2F_c^2)/3$, $S = 1.067$.

3.5. $[Os(SC_6F_5)_2(o\text{-}S_2C_6F_4)(PMe_2Ph)]$ (**2a**)

$C_{26}H_{11}F_{14}OsPS_4$, M = 938.76 monoclinic, space group $P2_1/n$, $a = 10.954(4)$, $b = 24.302(8)$, $c = 11.794(6)$ Å, $\alpha = 90$, $\beta = 110.95(3)$ $\gamma = 90°$, $U = 2932(2)$ Å^3, $Z = 4$, $T = 293(2)$ K, $D_c = 2.127$ g cm^{-3}, $F(000) = 1792$, μ(Mo–K$_\alpha$) = 4.797 mm^{-1}, λ(Mo–K$_\alpha$) = 0.71069 Å. The crystals are deep green. Intensity data were collected for a crystal of dimensions 0.20 × 0.10 × 0.05 mm mounted on a CAD4 diffractometer $\omega/1.66\theta$ mode with ω scan width = $0.80 + 0.34 \tan\theta$, ω scan speed 1.3–5.5° min^{-1}, graphite-monochromated Mo–K$_\alpha$ radiation. Of 3194 reflections collected, 3014 were independent. ψ-Scan absorption correction (max. and min. transmission: 99.9 and 74.3) giving 1517 with $I > 2\sigma(I)$. θ range for data collection: 2.16 to 21.00°, index ranges: $0 \leq h \leq 13$, $0 \leq k \leq 30$, $-14 \leq l \leq 13$. The structure was solved by direct methods [31] (most atoms) followed by difference Fourier synthesis and refined by full-matrix least-squares on F^2, using the SHELXL-93 program [30] with all non-hydrogen atoms anisotropic. The weighting scheme $w = [\sigma^2(F_o^2) + (0.0000P)^2 + 0.00P]^{-1}$ where $P = (\mathrm{Max}[F_o^2] + 2F_c^2)/3$. Final R indices with $I > 2\sigma(I)$: $R_1 = 0.0399$, $wR_2 = 0.0531$, and R indices, with all data $R_1 = 0.1473$, $wR_2 = 0.0684$.

3.6. $[Os(C_6F_5)_2(o\text{-}S_2C_6F_4)(PMe_2Ph)_2]$ (**3a**)

$C_{34}H_{22}F_{14}OsP_2S_2$, M = 1012.77, monoclinic, space group $P2_1/a$, $a = 16.2965(10)$, $b = 12.1332(10)$, $c = 18.854(3)$ Å, $\alpha = 90$, $\beta = 105.36(3)$, $\gamma = 90°$, $U = 3594.8(7)$ Å^3, $Z = 4$, $T = 293(2)$ K, $D_c = 1.871$ g cm^{-3}, $F(000) = 1960$, μ(Mo–K$_\alpha$) = 3.851 mm^{-1}, λ(Mo–K$_\alpha$) = 0.71069 Å. The crystals are red. Intensity data were collected for a crystal of dimensions 0.39 × 0.12 × 0.10 m^3 mounted on a CAD4 diffractometer $\omega/1.66\theta$ mode with ω scan width = $0.80 + 0.34 \tan\theta$, ω scan speed 1.3–5.5° min^{-1}, graphite-monochromated Mo–K$_\alpha$ radiation. Of 6529 reflections collected, 6324 were independent. ψ-Scan absorption correction (max. and min. transmission: 99.95 and 73.98) giving 1517 with $I > 2\sigma(I)$. θ range for data collection: 1.12–24.97°, index ranges: $-19 \leq h \leq 18$, $0 \leq k \leq 14$, $0 \leq l \leq 22$. The structure was solved by direct methods [31] (most atoms) followed by difference Fourier synthesis and refined by full-matrix least-squares on F^2, using the SHELXL-93 program [30] with all non-hydrogen atoms anisotropic. The weighting scheme $w = [\sigma^2(F_o^2) + (0.0338P)^2 + 0.00P]^{-1}$ where $P = (\text{Max}[F_o^2] + 2F_c^2)/3$. Final R indices with $I > 2\sigma(I)$: $R_1 = 0.0478$, $wR_2 = 0.0793$, and R indices, with all data $R_1 = 0.1365$, $wR_2 = 0.0934$.

4. Supplementary material

Crystallographic data (excluding structure factors) for the reported structures have been deposited at the Cambridge Crystallographic Data Centre with CCDC nos. 101739, 101740 and 101741 for compounds **1a**, **2a** and **3a**, respectively.

Acknowledgements

S.B. is grateful to UNAM for financial support and USAI for diffractometer time. We are grateful to Dr. Federico del Rio and Ing. L. Velasco (IQ) for help with the instrumentation and to DGAPA-UNAM, Mexico (IN121698), the European Union, CONACYT (25108E and 27915E) and CSIC, Spain, for financial support.

References

[1] B.L. Edelbach, B.M. Kraft, W.D. Jones, J. Am. Chem. Soc. 121 (1999) 10327.
[2] M.J. Atherton, J.H. Holloway, E.G. Hope, G.C. Saunders, J. Organomet. Chem. 558 (1998) 209.
[3] R. Bosque, E. Clot, S. Fantacci, F. Maseras, O. Eisenstein, R.N. Perutz, K.B. Renkema, K.G. Caulton, J. Am. Chem. Soc. 120 (1998) 12634.
[4] J. Fawcett, S. Friedrichs, J.H. Holloway, E.G. Hope, V. McKee, M. Nieuwenhuyzen, D.R. Russell, G.C. Saunders, J. Chem. Soc. Dalton Trans. (1998) 1477.
[5] M. Crespo, M. Martinez, E. de Pablo, J. Chem. Soc. Dalton Trans. (1997) 1231.
[6] L. Cronin, C.L. Higgitt, R. Karch, R.N. Perutz, Organometallics 16 (1997) 4920.
[7] B.L. Edelbach, W.D. Jones, J. Am. Chem. Soc. 119 (1997) 7734.
[8] R.P. Hughes, D.C. Lindner, J. Am. Chem. Soc. 119 (1997) 11544.
[9] A.N. Chernega, A.J. Graham, M.L.H. Green, J. Haggitt, J. Lloyd, C.P. Mehnert, N. Metzler, J. Souter, J. Chem. Soc. Dalton Trans. (1997) 2293.
[10] H. Plenio, Chem. Rev. 97 (1997) 5553.
[11] P. Murray-Rust, W.C. Stallings, C.T. Monti, R.K. Preston, J. Glusker, J. Am. Chem. Soc. 105 (1983) 3206.
[12] J. Burdeniuc, B. Jedlicka, R.H. Crabtree, Chem. Ber. 130 (1997) 145.
[13] J.L. Kiplinger, C.E. Osterberg, T.G. Richmond, Chem. Rev. 94 (1994) 373.
[14] R.H. Crabtree, Coord. Chem. Rev. 99 (1990) 89.
[15] R.M. Catala, D. Cruz Garritz, A. Hills, D.L. Hughes, R.L. Rychards, P. Sosa, and H. Torrens, J. Chem. Soc. Chem. Comm. (1987) 261.
[16] R.M. Catala, D. Cruz Garritz, P. Sosa, P. Terreros, H. Torrens, A. Hills, D.L. Hughes, R.L. Rychards, J. Organomet. Chem. 359 (1989) 219.
[17] M. Arroyo, S. Bernès, J.L. Brianso, R.L. Richards, J. Rius, H. Torrens, Inorg. Chem. Commun. 1 (1998) 273.
[18] L. Pauling, The Nature of the Chemical Bond, Third ed., Cornell, Ithaca, 1960.
[19] A. Bondi, J. Phys. Chem. 68 (1964) 441.
[20] M. Arroyo, D. Cruz-Garritz, A. Hills, D.L. Hughes, R.L. Richards, H. Torrens, J. Chem. Soc. Dalton Trans. (1991) 1281.
[21] M. Arroyo, J.A. Chamizo, D.L. Hughes, R.L. Richards, P. Sosa and H. Torrens, J. Chem. Soc. Dalton Trans. (1994) 1819.
[22] A.R. Rossi, R. Hoffmann, Inorg. Chem. 14 (1975) 365.
[23] P. Kalck, J.J. Bonnet, R. Poilblanc, J. Am. Chem. Soc. 104 (1982) 3069.
[24] M.J. Atherton, J. Fawcett, J.H. Holloway, E.G. Hope, A. Karaçar, D.R. Roussell, G.C. Saunders, J. Chem. Soc. Dalton Trans. (1996) 3215.
[25] F.H. Cano, P. Espinet, C. Foces-Foces, J. Fornies, A. Garcia, M Tomas, R. Uson, J. Organomet. Chem. 282 (1985) C35.
[26] S. Park, M. Pontier-Johnson, D.M. Roundhill, J. Am. Chem. Soc. 111 (1989) 3101.
[27] S. Park, M. Pontier-Johnson, D.M. Roundhill, Inorg. Chem. 29 (1990) 2689.
[28] J. Fawcett, E.G. Hope, L.A. Peck, Acta Crystallogr. Sect. C 54 (1998) 1752.
[29] F. Lahoz, E. Martin, J. Tiburcio, H. Torrens, P. Terreros, Trans. Metal Chem. 19 (1994) 381.
[30] G.M. Sheldrick, SHELXL-93. A Program for the Refinement of Crystal Structures from Diffraction Data.
[31] J. Rius, Acta Crystallogr. Sect. A 49 (1993) 406.